STUDY ON THE LARGE DEFORMATION MODULE IN FRAPTRAN 2.0

S.U. LEE*, H.C. Kim, Y.S. Yang and C.H. Shin

Nuclear Fuel Safety Division, Korea Atomic Energy Research Institute
111, Daedeok-daero 989 Beon-gil, Yuseong-gu, Daejeon, Republic of KOREA
** E-mail: sunguklee@kaeri.re.kr*

ABSTRACT

The FRAPTRAN code is used to simulate the behavior of the fuel rods in a transient state. Ballooning, which results in a large deformation of the clad within a short period of time, occurs during a LOCA. A BALON2 module of FRAPTRAN calculates the large deformation of the cladding. In the BALON2 module, the stress and strain at the node where the ballooning occurs are calculated with a perturbation theory, and the bowing effect of the cladding, and the temperature at that time, are recalculated. In this paper, various simulations were performed to evaluate factors such as the value of z_{bend} and time interval in the module, and compared with the data of the Halden-in-pile experiment. It has been shown that the mechanical behavior of the cladding is changed by the factors.

1. Introduction

Numerous operational and retrofit design changes were applied to LWRs after the loss of coolant accident (LOCA) at Three Mile Island. These specific design features and upgrades were primarily associated with maintaining adequate core cooling in the event that the primary cooling system is not functional. In particular, with a large cladding deformation, ballooning in LOCA leads to a flow blockage at the fuel assemblies. It is a very important phenomenon with respect to the loss of the core coolability. Fuel designers and safety authorities rely heavily on the fuel performance codes because they require minimal costs in comparison with the costs of an experiment or an unexpected fuel rod failure. The typical performance codes are FRAPCON and FRAPTRAN corresponding to the normal operation and the design-based accident (DBA) condition, respectively. As safety under DBA is of particular focus, there is a demand for the development and improvement of the performance code. In order to describe the ballooning phenomenon during a LOCA, the BALON2 module in FRAPTRAN2.0 [1] is applied.

There have been studies on changing the constitutive equations of the cladding tube at the BALON2 module in order to predict well the experimental results. Yadav et al. [2] developed a new performance code, TRAFR, using the creep model based on the existing FRAPTRAN2.0, and compared it with the experimental results. Plaez and Herranz [3] showed the large strain by changing the plastic model existing in the BALON2 module. In addition to the physical properties of the cladding material, it could be possible to change the deformation behavior by changing the parameters defined in the BALON2 module. For this purpose, we find the factors affecting the deformation in the BALON2 module and analyze how these affect the deformation.

2. BALON2 module at FRAPTRAN2.0 for large deformation

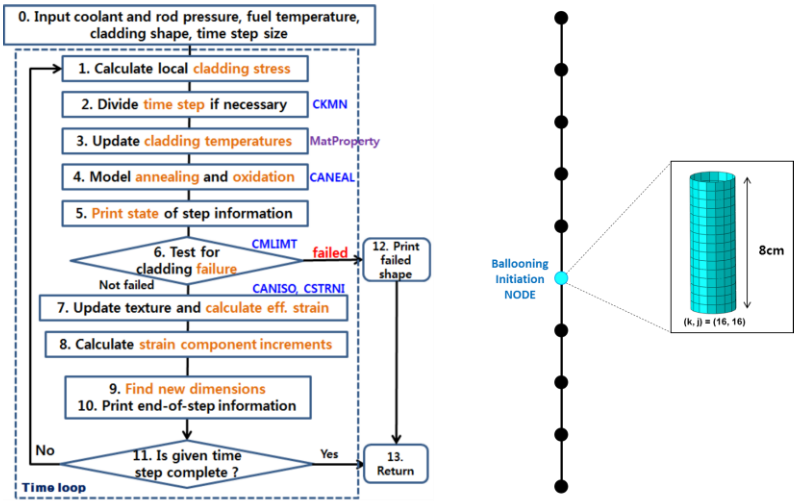

(a) (b)

Fig. 1. BALON2 module [4] (a) Flow-chart and (b) Simulation model

The Fuel Rod Analysis Program TRANsient (FRAPTRAN) is a Fortran language computer code that calculates the transient performance of light-water reactor fuel rods during reactor transients and hypothetical accidents such as LOCAs, anticipated transients without a scram, and Reactivity-Initiated Accidents (RIA). FRAPTRAN calculates the temperature and deformation history of a fuel rod as a function of the time-dependent fuel rod power and coolant boundary conditions. The deformation model at FRAPTRAN is a superposition of a one-dimensional radial and axial description, which is called the 1.5-D model or quasi 2-D model. The approximation using an axisymmetric, axially-stacked, 1-D radial representation saves computation cost. Based on the compatibility equations under axisymmetric and plane boundary conditions, the radial, circumferential, and axial components of the total strain for the cladding tube are derived.

BALON2 module at FRAPTRAN2.0 is used to express the ballooning deformation during LOCA. The perturbation theory is applied to calculate the stress of a large deformation in the module. The module is designed to take a bowing shape of the cladding tube. If the condition of the occurrence of ballooning is satisfied during the analysis of the performance code, the ballooning deformation is calculated based on the flowchart shown in Fig. 1 (a). First, local stresses are calculated using the pressure, temperatures, mid-wall radii, and wall thickness. Then, the given time step size is checked to see if it is short enough to prevent a significant change in the local stresses during the time step. The cladding temperatures are recalculated to account for the effects of the deformation during the previous time step in the cladding temperature. The effects of annealing are also considered for a flowchart. Next, all nodes are checked for a failure. The failure criteria at the BALON2 module is based on the stress of the clad. If a cladding failure has not occurred, the description of the cladding texture is updated and the effective strain prior to deformation is calculated. The dimension components are calculated from the effective strain and new dimensions at the end of the time step are defined under the assumption that a bending is applied. If there is a remaining part of the time step, the next time step proceeds with the previous calculated data. In the BALON2 module, a thermal-mechanics analysis is performed using a 16 x 16 cylindrical mesh, as shown in Figure 1 (b), which has node points of a fuel rod where ballooning begins. In this paper, the calculated result at the BALON2 module is visualized using PARAVIEW [5], which is open source.

2.1 Perturbation theory

In the FRACAS-I model, the hoop stress of the clad is calculated using the Thick-wall theory [6], as shown in Eq. (1). Through the perturbation theory, equation (2) of the hoop stress is expressed with the additional stress owing to the change in shape from the existing Eq. (1) [4]. In the BALON2 module, the third and fifth terms of Eq. (2) are ignored, assuming that the deformation calculations change into an axisymmetric shape.

$$\sigma_{\theta\theta} = \frac{P_i - P_o}{t_{ave}} r_{ave} - \frac{P_i + P_o}{2} \tag{1}$$

$$\sigma_{\theta\theta} = \frac{P_i - P_o}{t_{ave}} r_{ave} - \frac{P_i + P_o}{2} + \frac{P_i - P_o}{t_{ave}} \cancel{\delta} - r_{ave} \frac{\left(P_i - P_o\right)}{{t_{ave}}^2} h_\delta + \frac{P_i - P_o}{t_{ave}} \cancel{\frac{\partial^2 \delta}{\partial \theta_o^2}} + \frac{\sigma_{zz}}{\left(e^{\varepsilon_z}\right)^2} r_{ave} \frac{\partial^2 \delta}{\partial z_o^2}$$

$$\delta = r - r_{ave}, \quad h_\delta = t - t_{ave}, \quad \frac{\partial^2 \delta}{\partial \theta_o^2} = 0 \ for\, circle \tag{2}$$

2.2 Bending effect

Hagrman [4] described that the calculated radial displacement assumption through only perturbation theory did not match the data unless the failure stress was reduced by a factor of 0.6. He claimed that another assumption was needed to present the effect of bending due to different changes in cladding length during ballooning. To correct the difference between the experiment and the analysis, the code was written such that the position of the cladding was updated by bending, as shown in Fig. 2. By inputting the curvature value (Z_{bend}), as shown in Eq. 3, additional displacement due to bending could be imparted.

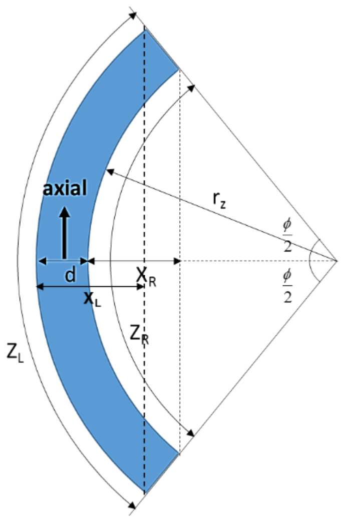

Fig. 2. Bowing shape of cladding tube due to bending

$$X_{ave} \approx \frac{{Z_{bend}}^2}{8r_0} \frac{\left[\exp\left(\varepsilon_{z_L}\right) - \exp\left(\varepsilon_{z_R}\right)\right]}{\left[\exp\left(\varepsilon_{\theta_R}\right) + \exp\left(\varepsilon_{\theta_L}\right)\right]} \tag{3}$$

3. Reference study with Halden-in-pile experiment (IFA 650.9)

3.1 Modelled IFA 650.9

Table 1 – Rod characteristics of IFA-650.9

Items	Value
Fuel - as fabricated and irradiated (AREVA)	
Initial enrichment [wt%U_{235}]	3.5
UO_2 density [g/cm^3]	10.43
Pellet diameter [mm]	9.131
Burnup [MWd/kgU]	89.9
Cladding - as fabricated and irradiated (AREVA)	
Type	Zry-4 (duplex cladding)
Outer diameter [mm]	10.75
Thickness [mm]	0.725
Outer liner [mm]	0.100
Oxide thickness, irradiated, mean [μm]	7
Hydrogen content, irradiated, ppm	30
After refabrication	
Fill gas / pressure [bar]	95% Ar + 5% He / 40
Free volume [cc]	19

To express the large strain in the LOCA situation, a high burnup (89.9 MWd/kgU) PWR fuel rod was used in the 9th LOCA test IFA-650.9, as a reference model. Because the cladding of the IFA650.9 test is a duplex type, which has low hydrogen contents, a large deformation is observed in spite of a high burnup fuel. The test segment was cut from a standard PWR fuel rod between spacers 2 and 3. This segment was a sibling rod to the one used for the previous test, IFA-650.4. It had been irradiated in the PWR Gösgen (Switzerland) during seven cycles (average cycle powers 325, 265, 290, 185, 175, 165 and 155 W/cm) and discharged in June 1998, as shown in figure 3. The length of the fuel stack was ~ 480 mm and no end pellets were inserted. The rod was filled with a gas mixture of 95 % argon and 5 % helium at 40 bars (RT) [7]. The characteristics of the fuel rod of IFA 650.9 are shown in Table 1. To simulate the transient behavior, the FRAPTRAN input is generated as follows: burnup data (FRAPCON file); gap gas of 95 % Ar; 5%He/ 40 bar@Room Temperature; simulation time of 0 to 500 s (time step, 0.01s); ALHR/Axial power shape, provided in DB; coolant pressure, provided in DB; HT oxidation of C-P model; and deformation of BALON2 model.

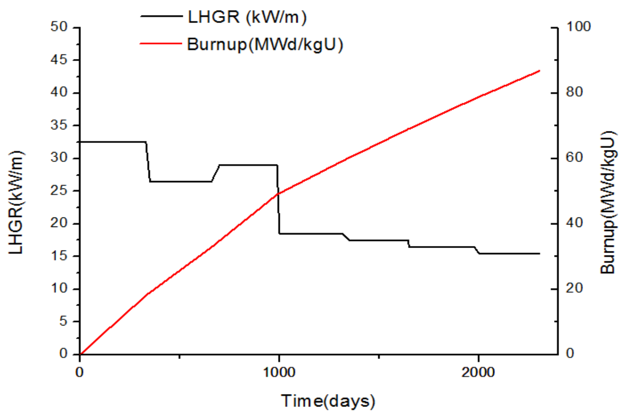

Fig. 3. LHGR and burnup build-up of IFA650.9 rod

The temperature of the clad and rod internal pressure measured in the experiment were used directly as input data to analyze only the characteristics of internal parameters affecting the mechanical deformation in the BALON2 module. For this, the measured values are sampled, as shown in Fig. 4.

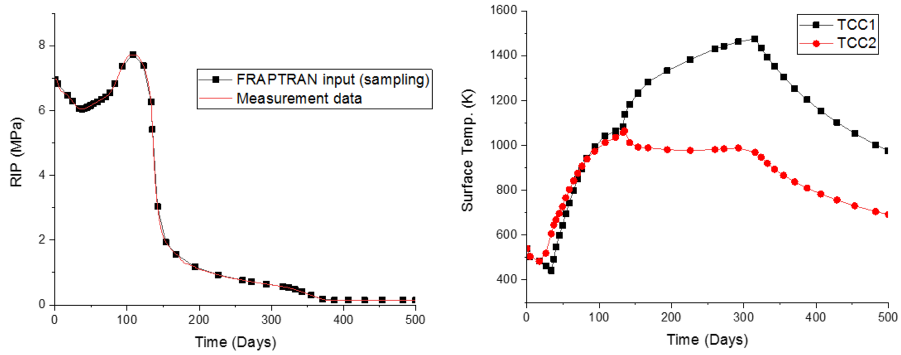

Fig. 4. Sampling data of IFA650.9, Rod internal gas pressure history (left), Surface temperature history of clad (right).

To determine whether the constructed FRAPTRAN model is valid, the simulation results from FRAPTRAN and the experimental results are compared in Fig. 5. Although there is a difference in the time of the burst, the results show good agreement against the measurement data.

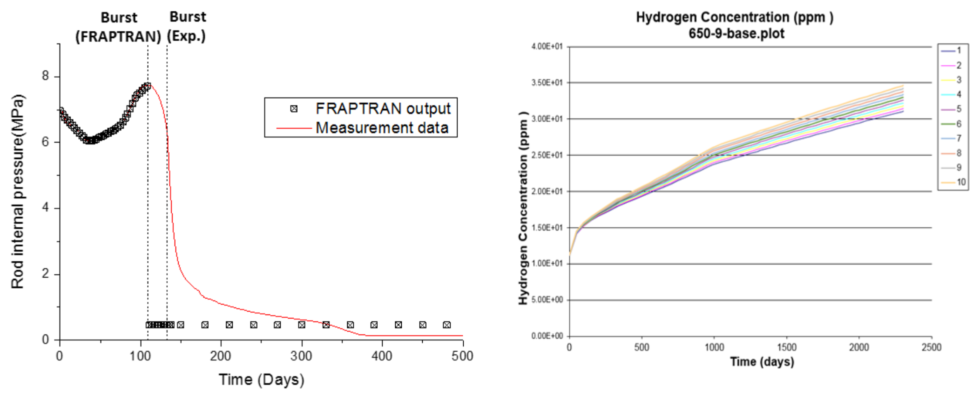

Fig. 5. Calculated Rod internal gas pressure (left) and hydrogen concentration (right) of IFA650.9

4. Results and Discussions

Based on the prepared IFA 650.9 input file, we analyzed the internal parameters affecting a large deformation. The internal factors include Z_{bend}, which reflects the bending effect, and the time increment in the deformation calculation.

4.1 Bending effect of cladding tube (Z_{bend})

The parameter, Z_{bend}, is the main factor used to express the bending effect of the cladding. The value of Z_{bend} is basically set to 0.1. To analyze the influence of Z_{bend}, the simulations were carried out with five Z_{bend} values (0.0, 0.05, 0.1, 0.15, 0.2). Looking at Figure 6, we can see that the value of Z_{bend} is affected when a failure occurs. However, it is not easy to analyze properly the influence of the parameter because of the limit of the pitch length. In order to analyze the change in the deformation behavior according to the Z_{bend} value, the pitch length restriction was released, and the analysis was performed again. Because there is no limitation, it is observed that various deformation behavior are shown in Fig. 7.

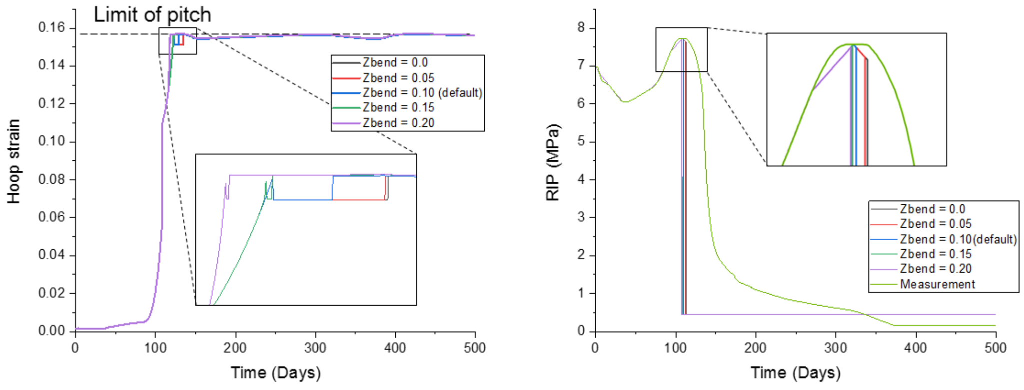

(a) (b)

Fig. 6. FRAPTRAN results according to the value of Z_{bend}: (a) hoop strain and (b) rod internal pressure.

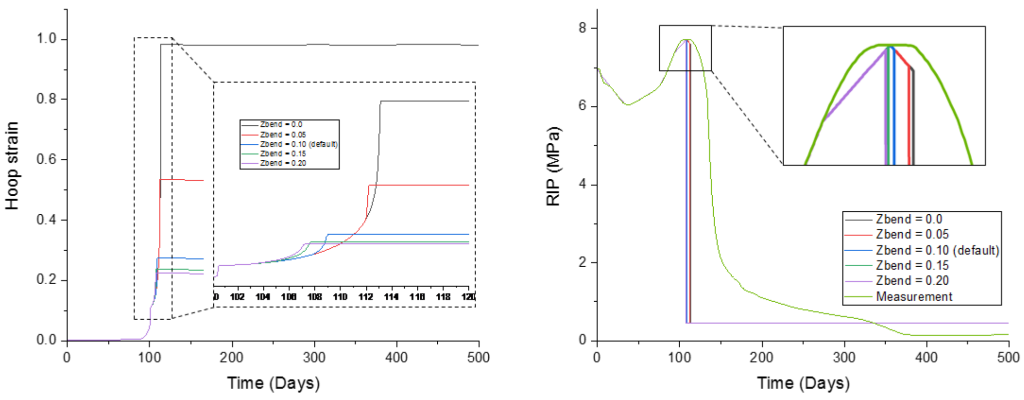

(a) (b)

Fig. 7. FRAPTRAN simulation results not considering the limit of the pitch: (a) hoop strain and (b) rod internal pressure.

The increasing slope of the strain depending on the value of Z_{bend} can be explained by the perturbation theory. The fraction (γ) of the hoop stress is defined as Eq. (4) to represent the effect of the perturbation theory,

$$\gamma = \frac{\sigma_{\theta\theta\_perturbation}}{\sigma_{\theta\theta\_total}} = \frac{-r_{ave}\dfrac{(P_i - P_o)}{t_{ave}{}^2}h_\delta + \dfrac{\sigma_{zz}}{\left(e^{\varepsilon_z}\right)^2}r_{ave}\dfrac{\partial^2\delta}{\partial z_o^2}}{\dfrac{P_i - P_o}{t_{ave}}r_{ave} - \dfrac{P_i + P_o}{2} - r_{ave}\dfrac{(P_i - P_o)}{t_{ave}{}^2}h_\delta + \dfrac{\sigma_{zz}}{\left(e^{\varepsilon_z}\right)^2}r_{ave}\dfrac{\partial^2\delta}{\partial z_o^2}} \tag{4}$$

In the calculation of the BALON2 module, this fraction (γ) was projected on the shape just before the rupture, and is shown in Fig. 8. When Z_{bend} is 0.0, the cladding tube is uniformly deformed in the circumferential direction. There is no thickness variation (h_δ=0) and no shape change ($\frac{\partial^2 \delta}{\partial Z_0^2}$=0) in the axial direction, and thus the value of the fraction approaches nearly zero. On the other hand, when the value of Z_{bend} is not zero, it was observed that a deviation occurs in the value of the circumferential radius. This leads to additional stresses by the perturbation theory, which affects the strain increase. As a result, it can be deduced that the strain increasing gradient is increased as Z_{bend} increases, as shown in Fig. 7.

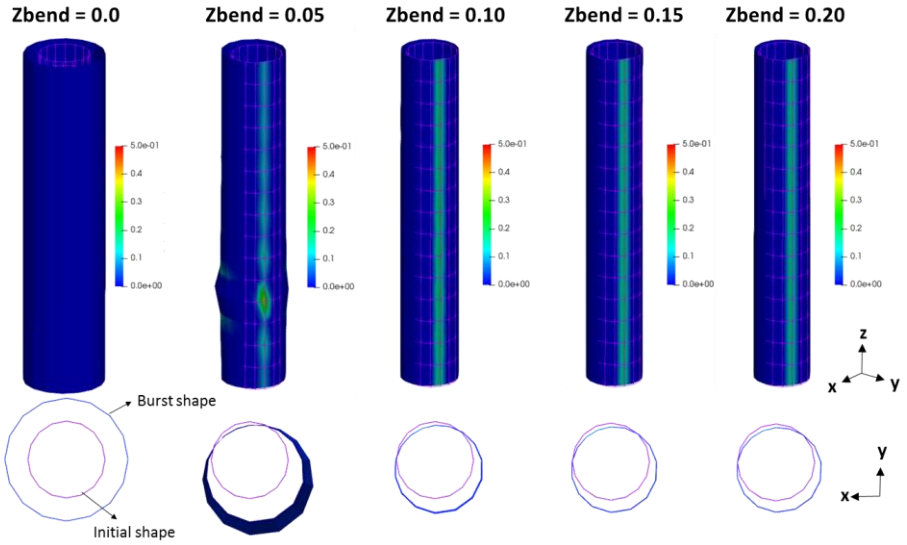

Fig. 8. Fraction (γ) of hoop stress by perturbation theory

It can be observed that as the Z_{bend} value increases, the failure rapidly occurs. The criteria for a rupture in FRAPTRAN apply both the strain and stress criteria, as shown in Fig. 9. In the BALON2 module, the failure criterion based on the stress is used. As the temperature of the clad increases, the criteria of the burst stress decreases.

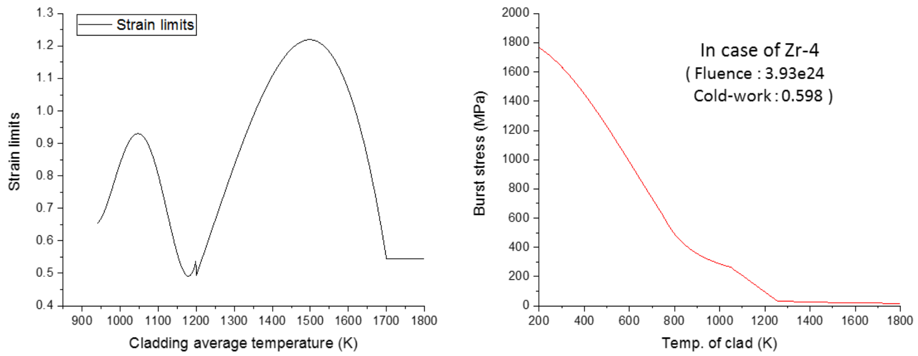

Fig. 9. Failure criteria of Zr-4 cladding tube, failure strain (left) and failure stress (right) [1].

As shown in Fig. 10, when Z_{bend} is zero, the gap between the pellet and the cladding tube is constant, which results in uniform cladding temperature. On the other hand, when bent, the gap between the pellet and cladding tube is reduced in the bent direction and the gap is increased in the opposite direction of the bending. A temperature deviation in the circumferential direction occurs. As the value of Z_{bend} increases, as shown in Fig. 10, it can be seen that the local maximum temperature is larger. As a result, the larger the Z_{bend} value is, the lower the criterion for the burst stress, the faster the rupture that occurs.

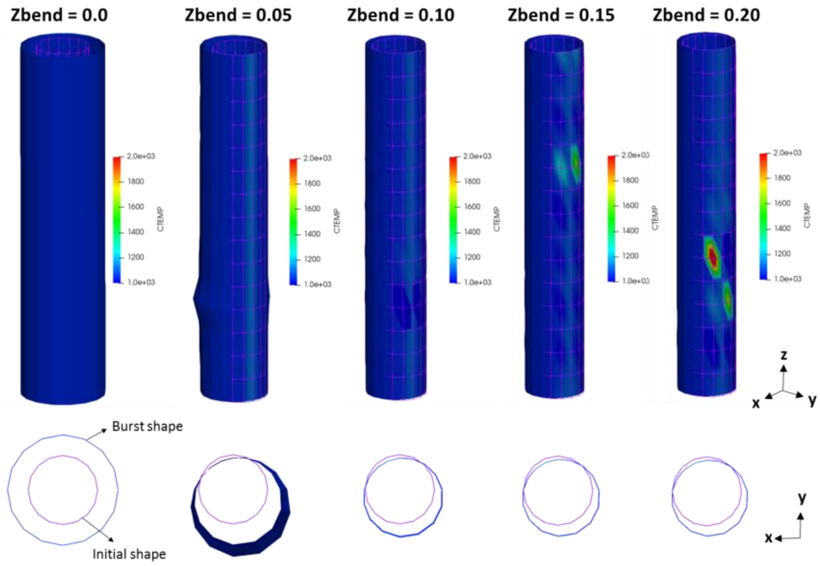

Fig. 10. Clad temperature and shape at ballooning region depending on the value of Z_{bend}.

4.2 Time increment (Δt)

Another factor affecting the large deformation during the computation is the time interval (Δt). At the BALON2 module, the time interval of each step is calculated based on the increment of the constant strain increment (Δε). Using the plastic yielding equation (5) of the cladding material, the time increment can be expressed as Equation (6). K, n, and m are defined according to the boundary conditions such as temperature and fluence. Once the strain increment (Δε) for each step is determined, the time increment (Δt) is automatically determined. In FRAPTRAN 2.0, the strain increment (Δε) is basically 0.01.

$$\bar{\sigma} = K\bar{\varepsilon}^{n}\left(\frac{\dot{\bar{\varepsilon}}}{10^{-3}}\right)^{m} \quad (5)$$

$$\Delta t = 10^{3}\left(\frac{K\varepsilon_{\theta}{}^{n}}{\sigma_{\theta}}\right)^{\frac{1}{m}} \cdot \Delta\varepsilon \quad (6)$$

To investigate the effect of deformation on the amount of strain increase, the analysis was carried out with strain increments of 0.001, 0.01, and 0.1. The results obtained are shown in Figs. 11 and 12. The same result can be obtained when the strain increment (Δε) is 0.01 or 0.1. However, when the increment amount is as small as 0.001, the hoop strain increases and the burst time is delayed, as shown in Fig. 12. In other words, as the amount of time increment (Δt) decreases, the hoop strain increases. In general, when calculating numerically using a nonlinear yield curve of metal, the yield slope becomes smaller. If the time increment is increased, the calculated stress value tends to be predicted larger than the real state. As a result, the calculated stress with a large time increment reaches the burst criteria of stress quickly. When the amount of strain increments is smaller, the more the strain that can be achieved until the rupture criterion is reached.

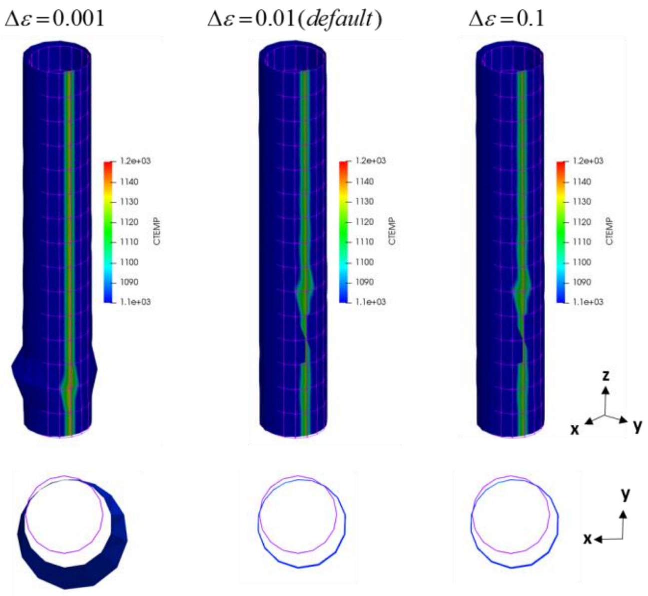

Fig. 11. Cladding temperature according to the strain increment.

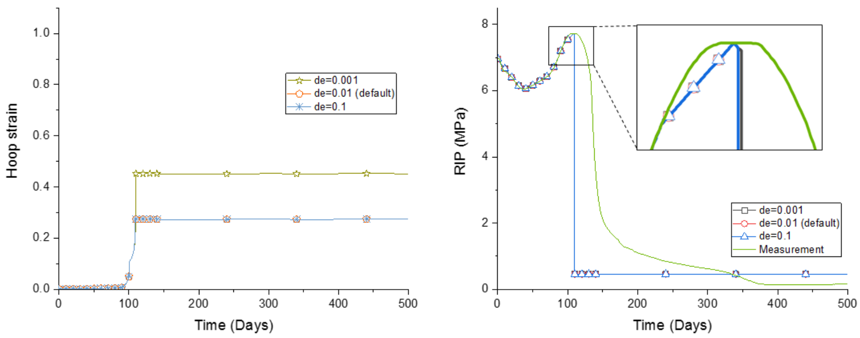

Fig. 12. FRAPTRAN2.0 results, hoop strain (left) and rod internal gas pressure (right) depending on the strain increment.

5. Conclusions

This paper was written to establish a working basis for the influence on the deformation by internal parameters except for the material characteristics in the BALON2 module. The sensitivity of each factor was evaluated through the input DB based on the IFA 650.9 test. The calculated bust strain varied from 0.22 to 0.98 due to the influence of the bending parameter, Z_{bend}. Depending on the time interval, the bust strain ranged from 0.27 to 0.45. It is seen that the internal parameters have a great influence on the deformation. The main insights can be summarized as follows.

1) Perturbation theory and a bending assumption are applied to express the ballooning phenomenon in the BALON2 module.
2) As the value of Z_{bend} increases, the local temperature increases. This causes rapid failure and reduces the value of the burst strain.
3) As the value of Z_{bend} increases, the slope of the hoop strain increases due to perturbation theory.
4) The larger the strain increment ($\Delta\varepsilon$) is for each step, the faster the burst occurs, and the

hoop strain decreases.

We plan to analyze the effect of the internal parameters in the BALON2 module through comparison with different halden test results (IFA 650.2 and 650.10).

ACKNOWLEDGMENT

This work has been carried out under the Nuclear R&D Program supported by the Ministry of Science & ICT (NRF-2017M2A8A4015024), Republic of Korea.

References

[1] K. J. Geelhood, W. G. Luscher, J.M. Cuta, I. A. Porter, FRAPTRAN-2.0 : A computer code for the transient Analysis of Oxide Fuel Rods, PNNL-19400, May, 2016..

[2] A.K. Yadav, C. Lee, S.U. Lee, C.H.Shin and H.Y. Kim, Numerical Simulation of Thermo-Mechanical coupled behavior of Clad tube under Intermediate Break LOCA, Proceeding of the 16th international Heat Transfer Conference, 2018.

[3] S.B. Pelaez and L.E. Herranz, Assessment of FRAPTRN modeling of Large Strain under Loss of Coolant Accidents, 2017 Water Reactor Fuel Performance Meeting, 2017.

[4] D. L. Hagrman, Zircaloy Cladding Shape at Failure (BALON2), Idaho National Engineering Laboratory, EGGCDAP-5379, July, 1981

[5] K. Moreland, PARAVIEW ver 5.2, Sandia National Lab.

[6] J.M. Gere and B.J. Goodno, Mechanics of Materials, Cengage Learning, 2008.

[7] F.B. du Chomont, LOCA Testing experiment at Halden. The nineth experiment IFA650-9. HWR 917, OECD Halden Reactor Project, 2009.